JPET Fast Forward. Published on October 8, 2009 as DOI: 10.1124/jpet.109.157750

JPET#157750

Title Page.

NF546 [4,4'-(carbonylbis(imino-3,1-phenylene-carbonylimino-3,1-(4-methyl-phenylene)-carbonylimino))-bis(1,3-xylene-α,α'-diphosphonic acid) tetrasodium salt] is a non-nucleotide $P2Y_{11}$ agonist and stimulates release of IL-8 from human monocyte-derived dendritic cells

Sabine Meis, Alexandra Hamacher, Darunee Hongwiset, Claudia Marzian, Michael Wiese, Niels Eckstein, Hans-Dieter Royer, Didier Communi, Jean-Marie Boeynaems, Ralf Hausmann, Günther Schmalzing, Matthias U. Kassack.

Primary laboratory of origin: Institute of Pharmaceutical and Medicinal Chemistry, Pharmaceutical Biochemistry, Heinrich-Heine-University of Duesseldorf, Universitaetsstr. 1, Building 26.23.01, D-40225 Duesseldorf, Germany (SM, AH, DH, MUK).

Institute of Pharmaceutical and Medicinal Chemistry, University of Bonn, An der Immenburg 4, D-53121 Bonn, Germany (CM, MW).

Institute of Human Genetics, University of Duesseldorf, Universitaetsstr. 1, D-40225 Duesseldorf, Germany (NE, HDR).

Institute of Interdisciplinary Research, IRIBHM – Faculty of Medicine, Université Libre de Bruxelles, 808 Route de Lennik, Campus Erasme, Building C 5th Floor, 1070 Brussels, Belgium (DC, JMB).

Molecular Pharmacology, RWTH Aachen University, Wendlingweg 2, D-52074 Aachen, Germany (RH, GS).

JPET Fast Forward. Published on October 8, 2009 as DOI: 10.1124/jpet.109.157750
This article has not been copyedited and formatted. The final version may differ from this version.

JPET#157750

Running Title Page

Running title:

Characterisation of the first non-nucleotide $P2Y_{11}$ agonist

Corresponding author:

Matthias U. Kassack, Institute of Pharmaceutical and Medicinal Chemistry, Pharmaceutical Biochemistry, Heinrich-Heine-University of Duesseldorf, Universitaetsstr. 1, Building 26.23.01, D-40225 Duesseldorf, Germany, Phone: +49-211-81 14587, Fax: +49-211-81 10801, e-mail: matthias.kassack@uni-duesseldorf.de

Number of text pages: 35

Number of tables: 3

Number of figures: 7

Number of references: 38

Number of words – abstract: 231

Number of words – introduction: 574

Number of words – discussion: 1203

Supplemental data: 1 table (Table S1)

Abbreviations:

ATPγS: adenosine-5'-O-(3-thio)triphosphate

ADPβS: adenosine-5'-*O*-(2-thio)diphosphate

BzATP: 2'-3'-*O*-(4-benzoylbenzoyl)-ATP

DC: human monocyte-derived dendritic cells

JPET Fast Forward. Published on October 8, 2009 as DOI: 10.1124/jpet.109.157750
This article has not been copyedited and formatted. The final version may differ from this version.

HRP: horseradish peroxidase

IL-4: interleukin 4

IL-8: interleukin 8

IL-12: interleukin 12

LPS: lipopolysaccharide

2-MeSATP: 2-(methylthio)adenosine-5′-triphosphate

TSP-1: thrombospondin-1

Recommended Section Assignment:

Cellular and Molecular

Abstract.

The G protein-coupled $P2Y_{11}$ receptor is involved in immune system modulation. In depth physiological evaluation is however hampered by a lack of selective and potent ligands. By screening a library of sulfonic and phosphonic acid derivatives at $P2Y_{11}$ receptors recombinantly expressed in human 1321N1 astrocytoma cells (calcium and cAMP assays), the selective non-nucleotide $P2Y_{11}$ agonist NF546 [4,4'-(carbonylbis(imino-3,1-phenylene-carbonylimino-3,1-(4-methyl-phenylene)carbonylimino))-bis(1,3-xylene-α,α'-diphosphonic acid) tetrasodium salt] was identified. NF546 had a pEC_{50} of 6.27 and is relatively selective for $P2Y_{11}$ over $P2Y_1$, $P2Y_2$, $P2Y_4$, $P2Y_6$, $P2Y_{12}$, $P2X_1$, $P2X_2$, and $P2X_2$-X_3. ATPγS, a non-hydrolysable analogue of the physiological $P2Y_{11}$ agonist ATP, and NF546 use a common binding site as suggested by molecular modelling studies and their competitive behaviour towards the nanomolar potency antagonist NF340 [4,4'-(carbonylbis(imino-3,1-(4-methyl-phenylene)carbonylimino))bis(naphthalene-2,6-disulfonic acid) tetrasodium salt] in Schild analysis. The pA_2 of NF340 was 8.02 against ATPγS and 8.04 against NF546 (calcium assays). NF546 was further tested for $P2Y_{11}$–mediated effects in monocyte-derived dendritic cells. Equal to ATPγS, NF546 led to thrombospondin-1 secretion and inhibition of LPS-stimulated IL-12 release, whereas NF340 inhibited these effects. It was further shown for the first time that ATPγS or NF546 stimulation promotes IL-8 release from dendritic cells which could be inhibited by NF340. In conclusion, we have described the first selective, non-nucleotide agonist NF546 for $P2Y_{11}$ receptors in both, recombinant and physiological expression systems and could show a $P2Y_{11}$–stimulated IL-8 release further supporting an immunomodulatory role of $P2Y_{11}$ receptors.

JPET Fast Forward. Published on October 8, 2009 as DOI: 10.1124/jpet.109.157750
This article has not been copyedited and formatted. The final version may differ from this version.

Introduction

P2-receptors are divided into ionotropic (ligand-gated ion channel) P2X and metabotropic (G protein-coupled) P2Y receptors. Up to now 8 subtypes of human P2Y receptors are cloned and characterized ($P2Y_{1, 2, 4, 6}$ and $_{11-14}$) (Abbracchio et al., 2006). P2 receptors play important roles in diverse (patho)-physiological processes as for example in the immune system (Di Virgilio et al., 2001;Marteau et al., 2005), platelet aggregation (Gachet, 2008), neurotransmission (Franke et al., 2006), oncology (White and Burnstock, 2006), inflammation and pain (Burnstock, 2004). P2Y-receptors are activated by nucleoside triphosphates, nucleoside diphosphates, and nucleotide-sugars (ATP, UTP, ADP, UTP, UDP-glucose). $P2Y_{1, 2, 4}$ and $_6$ receptors couple to G_q, whereas $P2Y_{12, 13}$ and $_{14}$ receptors couple to G_i. Only $P2Y_{11}$ receptors are coupled to both the cAMP and the phosphoinositide pathway (G_q and G_s) (Qi et al., 2001a). Since cloning and characterisation of the $P2Y_{11}$ receptor (Communi et al., 1997), a lot of knowledge has been gathered on multiple pharmacological actions of $P2Y_{11}$ receptors. Carriers of the Ala-87-Thr polymorphism of $P2Y_{11}$ receptors have an increased risk of acute myocardial infarction (Amisten et al., 2007). $P2Y_{11}$ receptors are (among other P2 receptors) involved in smooth muscle relaxations (King and Townsend-Nicholson, 2008). Swennen et al. reported that ATP inhibited tumor necrosis factor-alpha release via activation of $P2Y_{11}$ receptors (Swennen et al., 2008). A couple of studies were performed on the role of $P2Y_{11}$ receptors in human monocyte-derived dendritic cells. $P2Y_{11}$ receptors mediate ATP-induced semi-maturation of monocyte-derived dendritic cells (Wilkin et al., 2001). However, ATP effects on monocyte-derived dendritic cells are mediated by multiple P2Y receptors and also include effects of ADP as the ATP degradation product (Marteau et al., 2004). Marteau et al. reported on thrombospondin-1 (TSP-1) release from monocyte-derived dendritic cells upon ATP stimulation most likely mediated by $P2Y_{11}$ receptors, thus making $P2Y_{11}$ receptors potential targets for dendritic cell-based immunotherapy

JPET Fast Forward. Published on October 8, 2009 as DOI: 10.1124/jpet.109.157750
This article has not been copyedited and formatted. The final version may differ from this version.

(Marteau et al., 2005). $P2Y_{11}$ receptors furthermore play a role in the ATP-mediated inhibition of neutrophil apoptosis. Thus, specific targeting of $P2Y_{11}$ receptors could reduce neutrophil-mediated inflammatory processes (Vaughan et al., 2007).

ATP is the endogenous ligand at $P2Y_{11}$ receptors. In order to study in depth the contribution of $P2Y_{11}$ receptors, selective and potent ligands are required. So far, non-nucleotide and selective agonists and antagonists are lacking for $P2Y_{11}$ receptors except for NF157 and marine sponge-derived iantherans (Greve et al., 2007;Ullmann et al., 2005). NF157 was recently introduced by our group as an antagonist at $P2Y_{11}$ receptors, selective over $P2Y_1$ and $P2Y_2$ but not $P2X_1$. The iantherans are of limited availability due to their marine sponge origin. Naphthalene sulfonic acid urea derivatives have been an excellent source of selective and potent P2 receptor ligands (Braun et al., 2001;Damer et al., 1998;Kassack et al., 2004;Ullmann et al., 2005;Hausmann et al., 2006). We have thus performed a systematic screening of a compound library of naphthalene sulfonic and phosphonic acid urea derivatives for $P2Y_{11}$ receptor activation or inhibition using a fluorescence-based calcium assay (Kassack et al., 2002). This screen has resulted in the identification of NF340 [4,4'-(carbonylbis(imino-3,1-(4-methyl-phenylene)carbonylimino))bis(naphthalene-2,6-disulfonic acid) tetrasodium salt], a 4-fold more potent antagonist than NF157 and the first non-nucleotide $P2Y_{11}$ agonist NF546 [4,4'-(carbonylbis(imino-3,1-phenylene-carbonylimino-3,1-(4-methyl-phenylene)carbonylimino))-bis(1,3-xylene-α,α'-diphosphonic acid) tetrasodium salt] (Fig. 1). This paper describes the characterisation of the non-nucleotide agonist NF546 at $P2Y_{11}$ receptors recombinantly expressed in human 1321N1 astrocytoma cells and the modulation of cytokine release by NF340 and NF546 from human monocyte-derived dendritic cells. Now-available selective $P2Y_{11}$ ligands (NF546, NF340) allow in-depth physiological evaluation of the role of the $P2Y_{11}$ receptors.

JPET Fast Forward. Published on October 8, 2009 as DOI: 10.1124/jpet.109.157750
This article has not been copyedited and formatted. The final version may differ from this version.

Methods

Materials

All nucleotides (ATP, adenosine 5'-*O*-(3-thiotriphosphate) (ATPγS), adenosine 5'-*O*-(2-thiodiphosphate) (ADPβS), 2'-3'-*O*-(4-benzoylbenzoyl)-ATP (BzATP), UTP, UDP, ADP, 2-(methylthio)adenosine-5′-triphosphate (2-MeSATP)), lipopolysaccharide (LPS), forskolin and other reagents were obtained from Sigma-Aldrich, Taufkirchen, unless otherwise stated. Germany. NF340 and NF546 were synthesized according to methods previously published (Kassack et al., 2004;Ullmann et al., 2005). Structures of NF340 and NF546 (Fig. 1) were confirmed by ^{1}H- and ^{13}C-NMR. Purity was checked by CHN and HPLC and was > 95% (Kassack and Nickel, 1996). Synthesis will be published elsewhere. Molecular weights are: NF340: 986.83 g/mol; NF546: 1180.75 g/mol.

Cell culture and stable transfection of cells

Human 1321N1 astrocytoma cells were stably transfected with pcDNA3.1(+) vector (Invitrogen, Karlsruhe, Germany) containing the coding sequences of $P2Y_1$ (GenBank ACC# AY136752), $P2Y_2$ (GenBank ACC# AY136753), $P2Y_4$ (GenBank ACC# NM_002565), $P2Y_6$ (GenBank ACC# AF498920), $P2Y_{11}$ (**MAANVS**GAK-: GenBank ACC# AY449733 or **MDR**GAK-: GenBank ACC# AF030335), or $P2Y_{12}$ (GenBank ACC# NM_176876), respectively. All plasmids were from the Missouri S&T cDNA Resource Center (www.cdna.org) except for $P2Y_{11}$-MDRGAK which was from Communi et al. (Communi et al., 1997). Unless otherwise stated, $P2Y_{11}$ means the $P2Y_{11}$-**MAANVS**GAK clone. Cloned cell lines were cultured in Dulbecco´s modified Eagle Medium (DMEM) with sodium pyruvate, glucose (4500 mg/L), and pyridoxine supplemented with 5mM L-glutamine, 100 U/mL penicillin G, 100 µg/mL

JPET Fast Forward. Published on October 8, 2009 as DOI: 10.1124/jpet.109.157750
This article has not been copyedited and formatted. The final version may differ from this version.

streptomycin, 10% fetal bovine serum (Sigma-Aldrich), and 400 µg/mL G418 (Calbiochem). Cells were incubated at 37°C in a humidified atmosphere under 5% CO_2.

Measurements of intracellular calcium

Ca^{2+} fluorescence was measured as previously described using a fluorescence microplate reader with a pipettor system (NOVOstar®; BMG LabTech, Offenburg, Germany) (Kassack et al., 2002;Ullmann et al., 2005). The following (standard) agonists were used to stimulate the respective receptors: $P2Y_1$: 2-MeSADP (pEC_{50}: 8.46 ± 0.18); $P2Y_2$: UTP (pEC_{50}: 6.86 ± 0.05); $P2Y_4$: UTP (pEC_{50}: 7.69 ± 0.15); $P2Y_6$: UDP (pEC_{50}: 6.89 ± 0.12); $P2Y_{11}$: ATPγS (pEC_{50}: 7.26 ± 0.03). Concentration-inhibition curves of antagonists were obtained by preincubating the cells with test compounds for 30 min at 37°C and subsequent injection of agonist (31.6 nM 2-MeSADP ($P2Y_1$), 1 µM UTP ($P2Y_{2,\ 4}$), 1 µM UDP ($P2Y_6$), or 1 µM ATPγS ($P2Y_{11}$), respectively).

Analysis of cAMP levels

cAMP levels were estimated using a reporter-gene assay as recently described (Hamacher et al., 2006). 1321N1-$P2Y_{11}$ cells or 1321N1-$P2Y_{12}$ cells were transfected with 30 µg pCRE-luc (Stratagene, LaJolla, CA), using Polyfect (Qiagen, Hilden, Germany). 24 h after transfection, cells were split into two white 96-well plates (Greiner, Frickenhausen, Germany) and incubated in complete DMEM. 72 h after transfection, medium was replaced by phenol red- and serum-free DMEM:F12 media (1:1 mix). Cells were then stimulated with agonists or test compounds depending on their G_α-coupling. For $P2Y_{11}$ receptors, agonist screening was performed by a 3 h stimulation (37°C/5% CO_2) in the absence of forskolin. Compounds were tested for antagonism by preincubation for 30 min prior to addition of 1 µM ATPγS and 3 h incubation at 37°C in a 5%

JPET Fast Forward. Published on October 8, 2009 as DOI: 10.1124/jpet.109.157750
This article has not been copyedited and formatted. The final version may differ from this version.

CO_2 incubator. For $P2Y_{12}$ receptors, agonist screening was performed by 3 h stimulation (37°C/ 5% CO_2) in the presence of 10 µM forskolin. Compounds were tested for antagonism at $P2Y_{12}$ receptors by preincubation for 30 min prior to addition of 100 nM 2-MeSADP (pEC_{50}: 8.96 ± 0.14) and 10 µM forskolin and incubation for 3 h at 37°C in a 5% CO_2 incubator. After incubation, cells were lysed in 100 µL of lysis buffer (8 mM tricine, 2 mM EDTA, 1 mM DTT, 5% Triton, pH 7.8) and incubated for 20 min at 4°C in the dark. Luciferase activity was determined after adding 100 µl of luciferase-assay reagent (30 mM tricine, 10 mM $MgSO_4$, 0.5 mM EDTA, 10 mM DTT, 0.5 mM ATP, 0.5 mM coenzyme A, 0.5 mM D-luciferin) in a LUMIstar® microplate reader (BMG LabTech, Offenburg, Germany).

Electrophysiological evaluation at recombinant P2X receptors

The inhibitory or activating potency of NF340 and NF546 at P2X receptors was evaluated on X. laevis oocytes recombinantly expressing various rat P2X subtypes ($rP2X_1$, rPX_2, $rP2X_2$-X_3) using previously described protocols(Hausmann et al., 2006;Ullmann et al., 2005).

Preparation of human monocyte-derived dendritic cells

Immature human DCs were generated from adherent peripheral blood monocytes obtained from buffy coats of healthy volunteer donors as described previously (Romani et al., 1994;Wilkin et al., 2001). After 5 or 6 days of culture in the presence of 800 U/mL of granulocyte-macrophage colony-stimulating factor (GM-CSF; Invitrogen, Karlsruhe, Germany) and 500 U/mL of interleukin-4 (IL-4) (Invitrogen), cells were replated at 10^6 cells/mL in 24 multiwells in complete medium with GM-CSF and IL-4.

Stimulation of monocyte-derived dendritic cells for ELISA measurements

DCs were treated with NF546, ATPγS, or NF340 in the absence or in the presence of LPS (100 ng/mL) for 24 h. Supernatants of treated DCs were collected for measurements of cytokine profile and enzyme-linked immunosorbent assay (ELISA) measurements of thrombospondin-1 (TSP-1), and interleukin-8 and -12 (IL-8, IL-12p70).

Enzyme-linked immunosorbent assay (ELISA)

Human TSP-1 was measured using a commercially available ELISA kit from Chemicon International (Hampshire, United Kingdom). Human IL-8 and IL-12p70 were measured using commercially available kits from Pierce (Rockford, USA).

Measurement of cytokine and chemokine release

Human cytokines in cell culture supernatants of dendritic cells were measured using the Proteome Profiler™ human Cytokine Array Kit Panel A (R&D systems, Wiesbaden, Germany) according to the manufacturer's instructions. The kit consists of a nitrocellulose membrane containing 36 different anti-cytokine antibodies spotted in duplicate. In brief, membranes were blocked with blocking buffer at room temperature for 1 h. 1 mL of DC supernatants was mixed with a biotinylated detection antibody cocktail at room temperature and then inbubated with membranes overnight at 4°C. Arrays were then washed 3 times for 10 min and subsequently incubated with streptavidin-HRP for 30 minutes at room temperature and again washed. Next, arrays were exposed to peroxidase substrate (ECL Plus Western Blotting detection reagent, GE Healthcare, Freiburg, Germany) for 1 min before imaging using a LAS 3000 chemiluminescence reader (Fujifilm Corp., Kleve, Germany). Time of exposure was between 1 and 30 min.

Data analysis

JPET Fast Forward. Published on October 8, 2009 as DOI: 10.1124/jpet.109.157750
This article has not been copyedited and formatted. The final version may differ from this version.

Effects of single doses of agonists were expressed as percentage of the standard agonist control responses (31.6 nM 2-MeSADP ($P2Y_1$), 1 µM UTP ($P2Y_{2,4}$), 1 µM UDP ($P2Y_6$), or 1 µM ATPγS ($P2Y_{11}$), 100 nM 2-MeSADP ($P2Y_{12}$), respectively). Effects of single doses of antagonists were expressed as percent inhibition (= standard agonist response minus standard agonist response in the presence of antagonist). Apparent functional K_i values were calculated according to the equation of Cheng and Prusoff (Cheng and Prusoff, 1973):

$K_i = IC_{50} / (1+ L/EC_{50})$

where IC_{50} is the inhibitory concentration 50% of the antagonist, EC_{50} is the effective concentration 50% of the used agonist, and L is the molar concentration of the used agonist. IC_{50} values for antagonists and EC_{50} values for agonists were derived from -log concentration - effect (inhibition) curves where pooled normalized data were fitted to the nonlinear 4-parameter logistic equation (Prism 4.00, GraphPad Software, San Diego, CA). All experiments were performed in triplicate assays and repeated at least three times.

Receptor modeling

The crystallographic structure of bovine rhodopsin was used as a template to construct a homology model of the $hP2Y_{11}$ receptor with the MOE software package (Chemical Computing Group, Montreal, Canada). As the modeling algorithm tends to prefer compact packing, the resulting binding pocket is quite narrow beneath the long second extracellular loop. Thus, the best model obtained was refined by a molecular dynamics simulation in a 1-palmitoyl-2-oleoyl-phosphatidylcholine (POPC) membrane within physiological sodium chloride solution under periodic boundary conditions. All molecular dynamics calculations were performed using the GROMACS software (http://www.gromacs.org). After extensive minimization with steepest descent and conjugated derivatives algorithm the model was subjected to molecular dynamics

with restraints on the receptor coordinates to first equilibrate the membrane environment. The molecular dynamics simulation of the relaxed receptor model was carried out for a simulation time of 5 ns, monitoring the overall system energy to ensure stability of the system. Following this simulation of the unoccupied receptor, NF340 was docked into the resulting binding pocket using GOLD (Cambridge Crystallographic Database, Cambridge, UK) and the complex was subjected again to a short molecular dynamics simulation (500 ps). NF546 was docked into the putative binding pocket via superposition with NF340. After that, NF546 as well as the flexible side chains of the amino acids in the pocket and the first extracellular loop were subjected to an optimization procedure using the MOE Homology Modeling protocol. Molecular models shown in Fig. 7 were prepared using the UCSF Chimera package from the Resource for Biocomputing, Visualization, and Informatics at the University of California, San Francisco (supported by NIH P41 RR-01081).

JPET Fast Forward. Published on October 8, 2009 as DOI: 10.1124/jpet.109.157750
This article has not been copyedited and formatted. The final version may differ from this version.

Results

Before screening the naphthalene urea library at $P2Y_{11}$ receptors, we wanted to clarify if biological activities of agonists at both splice variants of the $P2Y_{11}$ receptor described by Communi et al. were comparable (Communi et al., 2001). Most publications use the **MDR**GAK splice variant originally reported by Communi et al. (Communi et al., 1997;Communi et al., 1999;Patel et al., 2001;Qi et al., 2001a;Qi et al., 2001b;White et al., 2003). However, the amino terminal sequence **MAANVS**GAK is the correct beginning of the non-chimeric $P2Y_{11}$ receptor, whereas the sequence **MDR**GAK represents the junction between the *SSF1* and *P2Y*$_{11}$ gene products. No significant differences were observed in the pEC_{50} values of different ATP-analogues at both receptor splice variants using fluorescence calcium measurements (supplemental data: Table S1). The rank-order of potency was the same for both splice variants and comparable to the previously published rank-order of potency at $P2Y_{11}$-**MDR**GAK receptors (ATPγS ≈ BzATP > ATP > ADPβS > 2MeSATP) (Communi et al., 1999). Based on these results, all further studies were performed with the $P2Y_{11}$-**MAANVS**GAK receptor.

Screening of the naphthalene sulfonic and phosphonic acid urea library at $P2Y_{11}$ receptors was performed using a fluorescence calcium assay (Kassack et al., 2002). This screen resulted in the discovery of the antagonist NF340 and the agonist NF546 (for structural formula see Fig. 1). The inhibition by 10 µM NF340 of a response induced with standard agonists at P2Y receptors is shown in Table 1 (standard agonist concentrations and pEC_{50} values of agonists are given in the Methods section). Data for $P2Y_{1, 2, 4, 6, 11}$ are based on calcium measurements whereas data for $P2Y_{12}$ were estimated measuring cAMP. As can be seen in Table 1, NF340 inhibited only the $P2Y_{11}$ receptor. Functional characterisation of NF340 at $P2Y_{11}$ receptors is shown in Fig. 2 in comparison to the recently described $P2Y_{11}$ antagonist NF157 (Ullmann et al., 2005). Apparent

JPET Fast Forward. Published on October 8, 2009 as DOI: 10.1124/jpet.109.157750
This article has not been copyedited and formatted. The final version may differ from this version.

functional K_i values were calculated from calcium measurements as follows (Fig. 2A): NF157: 75.3 nM; NF340: 19.2 nM. NF340 is thus ~4-fold more potent than NF157 (calcium assay). In the cAMP assay, apparent functional K_i values were as follows (Fig. 2B): NF157: 544.7 nM; NF340: 52.4 nM. cAMP studies leave NF340 about 10-fold more potent than NF157. NF340 has thus K_i values of similar range in calcium and cAMP inhibition experiments. The concentration-inhibition curves of NF340 (calcium and cAMP) displayed Hill coefficients not significantly different from unity. To further examine the mode of inhibition by NF340 of the ATPγS effect, concentration-response curves of ATPγS were monitored in the absence and presence of increasing concentrations of NF340 in the calcium assay. Fig. 2C shows the rightward shift of the concentration-response curves and Fig. 2D displays the resulting Schild analysis. The Schild plot is a straight line with a slope not significantly different from unity. We thus assume a competitive behaviour of NF340 at the $P2Y_{11}$ receptor. The pA_2 value was estimated as 8.02 ± 0.12 (mean ± SEM). The pA_2 of NF340 is in a similar range as the pK_i derived from the inhibition curve in Fig. 2 A (7.71 ± 0.07, mean ± SEM).

Next, the activation by NF546 of P2Y receptors was tested. Fig. 3A shows concentration-effect curves of NF546 at $P2Y_1$, $P2Y_2$, $P2Y_4$, $P2Y_6$, $P2Y_{11}$, and $P2Y_{12}$ receptors in comparison to ATPγS at $P2Y_{11}$ in calcium assays. Table 2 lists the corresponding pEC_{50} values of NF546. Fig. 3B shows the activation of the $P2Y_{11}$ receptor by NF546 compared to ATPγS in the cAMP assay. The pEC_{50} values for NF546 and ATPγS in the calcium assay were 6.27 ± 0.07 and 7.26 ± 0.03, respectively. In the cAMP assay, the following pEC_{50} values were obtained: NF546: 5.53 ± 0.03; ATPγS: 6.59 ± 0.04. pEC_{50} values determined in the calcium assay were higher than those in the cAMP assay. This is in agreement with findings published by Qi et al. (Qi et al., 2001a;Qi et al., 2001b). EC_{50} ratios of ATPγS and NF546 were however similar in the calcium (9.8) and cAMP

JPET Fast Forward. Published on October 8, 2009 as DOI: 10.1124/jpet.109.157750
This article has not been copyedited and formatted. The final version may differ from this version.

assay (11.5). The efficacy (upper plateau of the concentration-effect curve) of NF546 and ATPγS at $P2Y_{11}$ is not significantly different in both assays (Fig 3A and 3B). NF546 can thus be considered a full agonist at $P2Y_{11}$ with ~ 10-fold less potency than ATPγS. Besides strong activation of the $P2Y_{11}$ receptor, activation by NF546 of $P2Y_2$, $P2Y_6$, and to a lesser extent of $P2Y_{12}$ was observed (Fig. 3A, Table 2). The activation of $P2Y_2$ by NF546 shown in Fig. 3A suggests that NF546 is a full agonist at $P2Y_2$. However, NF546 is about 100-fold less potent at $P2Y_2$ receptors (pEC_{50}: 4.82; Table 2) than the physiological agonists UTP (pEC_{50}: 6.86; data not shown) or ATP (pEC_{50}: 6.74; data not shown). On the contrary, NF546 is only 2.5-fold less potent at $P2Y_{11}$ (pEC_{50} 6.27, Table 2) than the physiological agonist ATP (pEC_{50}: 6.67, Table S1). These data support relative selectivity of NF546 for $P2Y_{11}$.

Next, the specificity of NF546 for the $P2Y_{11}$ receptor was tested by addition of NF157, a recently described $P2Y_{11}$ antagonist (Ullmann et al., 2005). Fig. 3C shows the complete inhibition of the signals of 1 µM ATPγS and 10 µM NF546 by addition of 10 µM NF157. To further elucidate the binding behaviour of NF546 compared to ATPγS and NF340, a Schild analysis using NF546 and NF340 was performed in the calcium (Fig. 4A, B) and the cAMP assay (Fig. 4C, D). Fig. 4A and 4C show the rightward shift of the concentration-response curves of NF546 in the presence of increasing concentrations of NF340. The corresponding Schild analyses are displayed in Fig. 4B and 4D and show straight lines with slopes not significantly different from unity. pA_2 values for NF340 were estimated as 8.04 ± 0.27 (calcium) and 7.96 ± 0.25 (cAMP). Results of NF546 from calcium and cAMP studies are thus in agreement and confirmed the pA_2 value of NF340 determined with ATPγS in the calcium assay (Fig. 2D).

JPET Fast Forward. Published on October 8, 2009 as DOI: 10.1124/jpet.109.157750
This article has not been copyedited and formatted. The final version may differ from this version.

Selectivity of NF340 and NF546 for $P2Y_{11}$ over other P2Y receptors was already presented above (Tables 1 and 2, Fig. 3A). To test the selectivity for $P2Y_{11}$ over P2X receptors, NF340 and NF546 were evaluated for inhibition/activation of recombinant P2X receptors ($P2X_1$, $P2X_2$, $P2X_2$-X_3) by methods previously described (Ullmann et al., 2005;Hausmann et al., 2006). Up to 3 µM NF340 or NF546 showed less than 25% inhibition and no activation of control responses (data not shown). Furthermore, no inhibition by NF340 or NF546 of soluble potato-apyrase (grade VI, 0.04 U/ml, method published in (Horner et al., 2005)) was observed up to a concentration of 100 µM (data not shown).

Further experiments were undertaken to examine if the effect of NF546 was caused by a release of ATP. The effect of NF546 on $P2Y_{11}$-1321N1 astrocytoma cells was measured in the absence and the presence of soluble potato-apyrase in the calcium assay. The activity of NF546 was unaffected in the presence of soluble potato-apyrase (data not shown). This result corroborates a direct interaction of NF546 and the $P2Y_{11}$ receptor and rejects a release of ATP caused by NF546.

We next tested the physiological relevance of above findings in human monocyte-derived dendritic cells (DCs). Wilkin et al. have previously reported that $P2Y_{11}$ receptors mediate the ATP-induced semi-maturation in DCs (Wilkin et al., 2001). Activation of $P2Y_{11}$ receptors in DCs by ATP or ATPγS may be monitored by thrombospondin-1 (TSP-1) release as shown by Marteau et al. (Marteau et al., 2005). We have thus prepared DCs according to Wilkin et al. and Marteau et al. and tested NF340 and NF546 at DCs for changes in calcium signalling and TSP-1 secretion (Fig. 5). ATP, UTP, and NF546 gave a calcium signal in DCs (Fig. 5A). Since UTP gave no calcium signal at recombinant $P2Y_{11}$ receptors expressed in human 1321N1 astrocytoma cells

JPET Fast Forward. Published on October 8, 2009 as DOI: 10.1124/jpet.109.157750
This article has not been copyedited and formatted. The final version may differ from this version.

(data not shown), we assume that the UTP signal was mediated by $P2Y_2$ (or $P2Y_4$). Even though this is in contrast to the report from White et al. who found a UTP calcium signal at $P2Y_{11}$ receptors (White et al., 2003), our result that UTP gave no $P2Y_{11}$ signal fits very well to our data using the $P2Y_{11}$ selective antagonist NF340: whereas NF340 had no effect on the UTP response, the ATP signal could be blocked by NF340 to the level of the UTP response. Further, the NF546 signal could be completely blocked by NF340. The results from our laboratory nicely fit together: UTP is not an agonist at $P2Y_{11}$, ATP is an agonist at $P2Y_2$ and $P2Y_{11}$, NF546 is a selective $P2Y_{11}$ agonist, NF340 is a selective $P2Y_{11}$ antagonist. Functional effects of NF340 and NF546 in DCs were further confirmed by measuring TSP-1 secretion (Fig. 5B). TSP-1 secretion was equally stimulated by ATPγS and NF546. Further, agonist-induced TSP-1 secretion was completely blocked by 10 μM NF340.

Marteau et al. have further reported modulation of cytokine release from DCs stimulated with lipopolysaccharide (LPS) and ATP or ATP derivatives (Marteau et al., 2004). Among others, LPS-induced release of IL-12 was found to be modulated by ATP. This prompted us to perform a cytokine profiling of DCs stimulated with ATPγS and NF546, respectively. Interestingly, ATPγS and NF546 had no effect on the release of any cytokine available in the used human proteome profiler cytokine array kit (Panel A, R&D systems, Wiesbaden, Germany) except for IL-8. Fig. 6A shows a detail of the cytokine array, namely effects on IL-8 and IL-12p70. The next step was to examine LPS-induced IL-12p70 secretion, to quantify IL-8 secretion, and to test for modulating effects of NF340 and NF546 on IL-12p70 and IL-8 secretion by ELISA (Fig. 6B, 6C). LPS led to the expected secretion of IL-12p70 in DCs, and this effect could be inhibited by ATPγS and NF546 to control level. Furthermore, we could demonstrate that addition of NF340 to LPS and ATPγS or NF546-stimulated DCs was able to block the effect of ATPγS and NF546

JPET Fast Forward. Published on October 8, 2009 as DOI: 10.1124/jpet.109.157750
This article has not been copyedited and formatted. The final version may differ from this version.

back to the level of LPS alone (Fig. 6B). ATPγS and NF546-stimulated IL-8 secretion could also be inhibited to basal level by addition of 10 μM NF340.

In order to get an insight into the molecular interaction of the agonist NF546 with the $P2Y_{11}$ receptor in comparison to the antagonist NF340, we have constructed a homology model of the $P2Y_{11}$ receptor based on the crystallographic structure of bovine rhodopsin. The nanomolar potency antagonist NF340 fits well into the derived binding pocket of the homology model in the inactive state (Fig. 7A). Arg106 and Arg307 form hydrogen bonds to the sulfonic acid in position 6 of the first naphthalene ring. Arg268 seems to stabilize the sulfonic acid in position 6 of the second naphthalene ring. These findings are in accordance to site-directed mutagenesis studies which identified these residues as essential for agonist binding (Zylberg et al., 2007). Other charged amino acids in the pocket contribute to the binding of NF340 as e.g. Lys22, Arg103, and His265 which interact with other sulfonic acid groups. Arg184 forms a hydrogen bond to the carbonyl group of the urea of NF340, and Thr110 and Thr164 also seem to stabilize the sulfonic acid in position 2 of the second naphthalene ring. The agonist NF546 fits also well into the suggested binding pocket (Fig. 7B). Nevertheless, parts of the large molecule remain in the extracellular space. Table 3 summarises the amino acids in the putative $P2Y_{11}$ receptor binding pocket and their interaction with NF340 and NF546, respectively. Both ligands share some of the amino acid interactions (e.g., Arg103, Thr164, Arg184, Arg268). However, NF546 shows fewer interactions and cannot occupy the region between Trp32, Arg106, and Arg307 whereas NF546 forms an additional hydrogen bond with Glu186. This latter interaction of NF546 with Glu186 is not possible for the monomeric amine precursor of NF546 which is in accordance to a complete lack of activity of the monomeric precursor at $P2Y_{11}$. Similarly, the amine precursor of NF340

JPET Fast Forward. Published on October 8, 2009 as DOI: 10.1124/jpet.109.157750
This article has not been copyedited and formatted. The final version may differ from this version.

has no activity at $P2Y_{11}$ which again is in accordance to the suggested molecular interaction displayed in Fig. 7.

JPET Fast Forward. Published on October 8, 2009 as DOI: 10.1124/jpet.109.157750
This article has not been copyedited and formatted. The final version may differ from this version.

Discussion

Two different splice variants for the $P2Y_{11}$ receptor are described in the literature (Communi et al., 2001). Most publications used the **MDR**GAK splice variant representing the chimeric junction between the *SSF1* and *P2Y*$_{11}$ gene products (Communi et al., 1997;Communi et al., 1999;Patel et al., 2001;Qi et al., 2001a;Qi et al., 2001b;White et al., 2003). In order to compare our data using the non-chimeric $P2Y_{11}$-**MAANVS**GAK receptor with literature data using the **MDR**GAK splice variant, we could show that the differences in the amino terminus did not lead to differences in the potency of nucleotide agonists (supplemental data Table S1). This allows to directly comparing data obtained with the different splice variants.

The purpose of this study was to characterise the non-nucleotide $P2Y_{11}$ agonist NF546 identified through a screening of sulfonic and phosphonic acid derivatives. The $P2Y_{11}$ receptor seems to play diverse interesting physiological roles which are however not fully explored due to a lack of appropriate ligands (Amisten et al., 2007;King and Townsend-Nicholson, 2008;Marteau et al., 2004;Marteau et al., 2005;Swennen et al., 2008;Vaughan et al., 2007;Wilkin et al., 2001). Previously, the non-selective inhibitor suramin was used as a starting point for synthetic variations of the methyl group resulting in the discovery of NF157, the first $P2Y_{11}$ antagonist with an apparent K_i of 75 nM in this study (Fig. 2A) and a pA_2 of 7.77 (Ullmann et al., 2005). NF157 has several disadvantages. It is not fully selective among P2 receptors, it is a rather large molecule containing six sulfonic acid groups, and the potency could be improved. However, the concept of searching among sulfonic acid group containing compounds turned out to be a fruitful approach in several P2 projects (Kassack et al., 2004;Lambrecht et al., 2002;Ullmann et al., 2005;Horner et al., 2005). We have thus undertaken the approach to search in a library of sulfonic and phosphonic acid compounds for $P2Y_{11}$ ligands using a widely applicable calcium

JPET Fast Forward. Published on October 8, 2009 as DOI: 10.1124/jpet.109.157750
This article has not been copyedited and formatted. The final version may differ from this version.

assay (Kassack et al., 2002). This strategy was successful. We discovered the competitive $P2Y_{11}$ antagonist NF340 which is selective for $P2Y_{11}$ among all tested P2 receptors and 4-fold more potent than NF157 (calcium assay, Fig. 2A). Inhibition by 10 µM NF340 of standard agonist responses at other P2Y receptors was less than 10%, corresponding to K_i values greater than 10 µM (Table 1). This leaves NF340 at least 520-fold selective for $P2Y_{11}$ over $P2Y_1$, $P2Y_2$, $P2Y_4$, $P2Y_6$, and $P2Y_{12}$ receptors. Further at $P2X_1$, $P2X_2$, and $P2X_{2-3}$ receptors, 3 µM NF340 produced no significant inhibition (data not shown), thus leaving NF340 at least 156-fold selective for $P2Y_{11}$.

Most interestingly, the screening approach led to the discovery of the non-nucleotide $P2Y_{11}$ agonist NF546 displaying the same efficacy as ATPγS (Fig. 3). NF546 has some structural features of NF157, the previously developed $P2Y_{11}$ antagonist (Ullmann et al., 2005), except for the lack of naphthalene sulfonic acid groups. Thus, the switch from antagonism to agonism lies in the exchange of naphthalene sulfonic acid groups (in NF157) to benzylic phosphonic acid groups in NF546. ATPγS is still about one order of magnitude more potent than NF546, but NF546 is only 2.5-fold less potent than ATP, the physiological $P2Y_{11}$ ligand. At $P2Y_2$ receptors, NF546 seems to be a full agonist, too (Fig. 3A) but remains 83-fold less potent than the physiological agonist ATP. The ratios of EC_{50} values for NF546 determined for activation of various P2Y receptors expressed in different stable cell lines with $P2Y_{11}$ receptors differ by at least 28-fold (Table 2). Further, up to 3 µM NF546 had no effect at the tested $P2X_1$, $P2X_2$, and $P2X_{2-3}$ receptors. Thus, in contrast to ATP which is a non-selective agonist for P2 receptors, NF546 shows relative selectivity for $P2Y_{11}$ over all tested P2Y and P2X receptors.

JPET Fast Forward. Published on October 8, 2009 as DOI: 10.1124/jpet.109.157750
This article has not been copyedited and formatted. The final version may differ from this version.

Taken together, these data support the advantage of NF546 over ATP or derivatives thereof. NF546 is only slightly less potent than ATP at $P2Y_{11}$ (2.5-fold) but much more selective for $P2Y_{11}$ over other P2 receptors and NF546 cannot be hydrolysed by nucleotidases due to its benzylic phosphonic acid structure. Ecke et al. have recently described $P2Y_{11}$-selective ATP derivatives (Ecke et al., 2006). The advantage of NF546 over these ATP derivatives is that NF546 can be chemically modified similar to the antiviral drug tenofovir to become bioavailable (Holy, 2003). This gives an additional value to this non-nucleotide agonist of $P2Y_{11}$ receptors.

We have not only discovered the antagonist NF340 and agonist NF546 but also explored their nature of interaction with the $P2Y_{11}$ receptor. NF340 is a competitive antagonist as shown in Schild analysis against ATPγS (Fig. 2) and it is also a competitive antagonist against NF546 (Schild analyses in Fig. 4). pA_2 values of NF340 were basically identical (~ 8) when using ATPγS or NF546 in calcium or cAMP assays, respectively (Figs. 2D, 4B, 4D). Since NF340 and NF546 are competitive and use the same binding pocket, we were interested to understand the binding mode at the molecular level. Docking of NF340 and NF546 into the binding pocket of the $P2Y_{11}$ receptor model and molecular dynamics simulations with NF340 resulted in a reasonable binding mode showing a large overlap of the NF340 and NF546 putative binding site (Fig. 7). Amino acids shown to be important for ligand binding and receptor activation form interactions, particularly hydrogen bonds and ionic interactions, throughout the simulation time, supporting the assumption of a competitive binding mode of NF340 and NF546 or the physiological agonist ATP (Table 3). Our findings are in accordance with site-directed mutagenesis studies which identified these residues as essential for agonist binding (Zylberg et al., 2007). Of particular importance is Arg268. The mutation of Arg268Ala reduced the potency of ATP by three orders of magnitude (Zylberg et al., 2007).

Most important, NF340 and NF546 were not only active at recombinant $P2Y_{11}$ receptors expressed in 1321N1 cells but also at native $P2Y_{11}$ receptors in monocyte-derived dendritic cells. DCs are known to express $P2Y_{11}$ receptors (Schnurr et al., 2003;Wilkin et al., 2001). NF546 and ATPγS were equi-efficacious in stimulating TSP-1 release (Fig. 5B) and inhibiting the LPS-induced release of IL-12p70 (Fig. 6B). Both release of TSP-1 and inhibition of LPS-induced release of IL-12p70 were previously reported to result from $P2Y_{11}$ receptor activation (Marteau et al., 2004;Marteau et al., 2005). Moreover, release of some cytokines by DCs upon stimulation with nucleotides has been studied by Marcet et al. (Marcet et al., 2007). To get a comprehensive picture of cytokine release from DCs stimulated with ATPγS or NF546, we used a human proteome profiler cytokine array (Fig. 6A). We discovered the release of IL-8 upon ATPγS and NF546 stimulation which was confirmed by ELISA and could be inhibited by the $P2Y_{11}$ selective antagonist NF340 (Figs. 6A, 6C). We have thus reported for the first time the release of IL-8 upon $P2Y_{11}$ stimulation in DCs by using our novel $P2Y_{11}$ selective ligands NF340 and NF546. These findings may have impact on strategies to modulate immune system reactions.

In conclusion, we have introduced the $P2Y_{11}$ antagonist NF340 with improved potency and selectivity compared to NF157 and the non-nucleotide $P2Y_{11}$ agonist NF546. These two compounds show functional effects in DCs and helped to discover the previously unknown IL-8 release upon $P2Y_{11}$ stimulation. These ligands will be helpful for further exploration of the physiological role of $P2Y_{11}$ receptors.

References

Abbracchio MP, Burnstock G, Boeynaems J M, Barnard E A, Boyer J L, Kennedy C, Knight G E, Fumagalli M, Gachet C, Jacobson K A and Weisman G A (2006) International Union of Pharmacology LVIII: Update on the P2Y G Protein-Coupled Nucleotide Receptors: From Molecular Mechanisms and Pathophysiology to Therapy. *Pharmacol Rev* **58**:281-341.

Amisten S, Melander O, Wihlborg A K, Berglund G and Erlinge D (2007) Increased Risk of Acute Myocardial Infarction and Elevated Levels of C-Reactive Protein in Carriers of the Thr-87 Variant of the ATP Receptor P2Y11. *Eur Heart J* **28**:13-18.

Braun K, Rettinger J, Ganso M, Kassack M, Hildebrandt C, Ullmann H, Nickel P, Schmalzing G and Lambrecht G (2001) NF449: a Subnanomolar Potency Antagonist at Recombinant Rat P2X1 Receptors. *Naunyn Schmiedebergs Arch Pharmacol* **364**:285-290.

Burnstock G (2004) Introduction: P2 Receptors. *Curr Top Med Chem* **4**:793-803.

Cheng Y and Prusoff W H (1973) Relationship Between the Inhibition Constant (K1) and the Concentration of Inhibitor Which Causes 50 Per Cent Inhibition (I50) of an Enzymatic Reaction. *Biochem Pharmacol* **22**:3099-3108.

Communi D, Govaerts C, Parmentier M and Boeynaems J M (1997) Cloning of a Human Purinergic P2Y Receptor Coupled to Phospholipase C and Adenylyl Cyclase. *J Biol Chem* **272**:31969-31973.

Communi D, Robaye B and Boeynaems J M (1999) Pharmacological Characterization of the Human P2Y11 Receptor. *Br J Pharmacol* **128**:1199-1206.

Communi D, Suarez-Huerta N, Dussossoy D, Savi P and Boeynaems J M (2001) Cotranscription and Intergenic Splicing of Human P2Y11 and SSF1 Genes. *J Biol Chem* **276**:16561-16566.

Damer S, Niebel B, Czeche S, Nickel P, Ardanuy U, Schmalzing G, Rettinger J, Mutschler E and Lambrecht G (1998) NF279: a Novel Potent and Selective Antagonist of P2X Receptor-Mediated Responses. *Eur J Pharmacol* **350**:R5-R6.

Di Virgilio F, Chiozzi P, Ferrari D, Falzoni S, Sanz J M, Morelli A, Torboli M, Bolognesi G and Baricordi O R (2001) Nucleotide Receptors: an Emerging Family of Regulatory Molecules in Blood Cells. *Blood* **97**:587-600.

Ecke D, Tulapurkar M E, Nahum V, Fischer B and Reiser G (2006) Opposite Diastereoselective Activation of P2Y1 and P2Y11 Nucleotide Receptors by Adenosine 5'-O-(Alpha-Boranotriphosphate) Analogues. *Br J Pharmacol* **149**:416-423.

Franke H, Krugel U and Illes P (2006) P2 Receptors and Neuronal Injury. *Pflugers Arch* **452**:622-644.

Gachet C (2008) P2 Receptors, Platelet Function and Pharmacological Implications. *Thromb Haemost* **99**:466-472.

Greve H, Meis S, Kassack M U, Kehraus S, Krick A, Wright A D and Konig G M (2007) New Iantherans From the Marine Sponge Ianthella Quadrangulata: Novel Agonists of the P2Y(11) Receptor. *J Med Chem* **50**:5600-5607.

Hamacher A, Weigt M, Wiese M, Hoefgen B, Lehmann J and Kassack M U (2006) Dibenzazecine Compounds With a Novel Dopamine/5HT2A Receptor Profile and 3D-QSAR Analysis. *BMC Pharmacol* **6**:11.

Hausmann R, Rettinger J, Gerevich Z, Meis S, Kassack M U, Illes P, Lambrecht G and Schmalzing G (2006) The Suramin Analog 4,4',4",4"'-(Carbonylbis(Imino-5,1,3-Benzenetriylbis (Carbonylimino)))Tetra-Kis-Benzenesulfonic Acid (NF110) Potently Blocks P2X3 Receptors: Subtype Selectivity Is Determined by Location of Sulfonic Acid Groups. *Mol Pharmacol* **69**:2058-2067.

Holy A (2003) Phosphonomethoxyalkyl Analogs of Nucleotides. *Curr Pharm Des* **9**:2567-2592.

Horner S, Menke K, Hildebrandt C, Kassack M U, Nickel P, Ullmann H, Mahaut-Smith M P and Lambrecht G (2005) The Novel Suramin Analogue NF864 Selectively Blocks P2X1 Receptors in Human Platelets With Potency in the Low Nanomolar Range. *Naunyn Schmiedebergs Arch Pharmacol* **372**:1-13.

Kassack M and Nickel P (1996) Rapid, Highly Sensitive Gradient Narrow-Bore High-Performance Liquid Chromatographic Determination of Suramin and Its Analogues. *J Chromatogr B Biomed Appl* **686**:275-284.

Kassack MU, Braun K, Ganso M, Ullmann H, Nickel P, Boing B, Muller G and Lambrecht G (2004) Structure-Activity Relationships of Analogues of NF449 Confirm NF449 As the Most Potent and Selective Known P2X1 Receptor Antagonist. *Eur J Med Chem 2004 Apr;39 (4):345 - 57* **39**:345-357.

Kassack MU, Hofgen B, Lehmann J, Eckstein N, Quillan J M and Sadee W (2002) Functional Screening of G Protein-Coupled Receptors by Measuring Intracellular Calcium With a Fluorescence Microplate Reader. *J Biomol Screen* **7**:233-246.

King BF and Townsend-Nicholson A (2008) Involvement of P2Y1 and P2Y11 Purinoceptors in Parasympathetic Inhibition of Colonic Smooth Muscle. *J Pharmacol Exp Ther* **324**:1055-1063.

Lambrecht G, Braun K, Damer M, Ganso M, Hildebrandt C, Ullmann H, Kassack M U and Nickel P (2002) Structure-Activity Relationships of Suramin and Pyridoxal-5'-Phosphate Derivatives As P2 Receptor Antagonists. *Curr Pharm Des* **8**:2371-2399.

Marcet B, Horckmans M, Libert F, Hassid S, Boeynaems J M and Communi D (2007) Extracellular Nucleotides Regulate CCL20 Release From Human Primary Airway Epithelial Cells, Monocytes and Monocyte-Derived Dendritic Cells. *J Cell Physiol* **211**:716-727.

Marteau F, Communi D, Boeynaems J M and Suarez G N (2004) Involvement of Multiple P2Y Receptors and Signaling Pathways in the Action of Adenine Nucleotides Diphosphates on Human Monocyte-Derived Dendritic Cells. *J Leukoc Biol* **76**:796-803.

Marteau F, Gonzalez N S, Communi D, Goldman M, Boeynaems J M and Communi D (2005) Thrombospondin-1 and Indoleamine 2,3-Dioxygenase Are Major Targets of Extracellular ATP in Human Dendritic Cells. *Blood* **106**:3860-3866.

Patel K, Barnes A, Camacho J, Paterson C, Boughtflower R, Cousens D and Marshall F (2001) Activity of Diadenosine Polyphosphates at P2Y Receptors Stably Expressed in 1321N1 Cells. *Eur J Pharmacol* **430**:203-210.

Qi AD, Kennedy C, Harden T K and Nicholas R A (2001a) Differential Coupling of the Human P2Y(11) Receptor to Phospholipase C and Adenylyl Cyclase. *Br J Pharmacol* **132**:318-326.

Qi AD, Zambon A C, Insel P A and Nicholas R A (2001b) An Arginine/Glutamine Difference at the Juxtaposition of Transmembrane Domain 6 and the Third Extracellular Loop Contributes to the Markedly Different Nucleotide Selectivities of Human and Canine P2Y11 Receptors. *Mol Pharmacol* **60**:1375-1382.

Romani N, Gruner S, Brang D, Kampgen E, Lenz A, Trockenbacher B, Konwalinka G, Fritsch P O, Steinman R M and Schuler G (1994) Proliferating Dendritic Cell Progenitors in Human Blood. *J Exp Med* **180**:83-93.

Schnurr M, Toy T, Stoitzner P, Cameron P, Shin A, Beecroft T, Davis I D, Cebon J and Maraskovsky E (2003) ATP Gradients Inhibit the Migratory Capacity of Specific Human Dendritic Cell Types: Implications for P2Y11 Receptor Signaling. *Blood 2003 Jul 15 ;102 (2):613 -20 Epub 2003 Mar 20* **102**:613-620.

Swennen EL, Coolen E J, Arts I C, Bast A and Dagnelie P C (2008) Time-Dependent Effects of ATP and Its Degradation Products on Inflammatory Markers in Human Blood Ex Vivo. *Immunobiology* **213**:389-397.

Ullmann H, Meis S, Hongwiset D, Marzian C, Wiese M, Nickel P, Communi D, Boeynaems J M, Wolf C, Hausmann R, Schmalzing G and Kassack M U (2005) Synthesis and Structure-Activity Relationships of Suramin-Derived P2Y11 Receptor Antagonists With Nanomolar Potency. *J Med Chem* **48**:7040-7048.

Vaughan KR, Stokes L, Prince L R, Marriott H M, Meis S, Kassack M U, Bingle C D, Sabroe I, Surprenant A and Whyte M K (2007) Inhibition of Neutrophil Apoptosis by ATP Is Mediated by the P2Y11 Receptor. *J Immunol* **179**:8544-8553.

White N and Burnstock G (2006) P2 Receptors and Cancer. *Trends Pharmacol Sci* **27**:211-217.

White PJ, Webb T E and Boarder M R (2003) Characterization of a Ca2+ Response to Both UTP and ATP at Human P2Y11 Receptors: Evidence for Agonist-Specific Signaling. *Mol Pharmacol* **63**:1356-1363.

Wilkin F, Duhant X, Bruyns C, Suarez-Huerta N, Boeynaems J M and Robaye B (2001) The P2Y11 Receptor Mediates the ATP-Induced Maturation of Human Monocyte-Derived Dendritic Cells. *J Immunol* **166**:7172-7177.

Zylberg J, Ecke D, Fischer B and Reiser G (2007) Structure and Ligand-Binding Site Characteristics of the Human P2Y11 Nucleotide Receptor Deduced From Computational Modelling and Mutational Analysis. *Biochem J* **405**:277-286.

Footnotes

a) This project was financially supported by the Deutsche Forschungsgemeinschaft DFG [Graduiertenkolleg GRK677] and by a stipend from the Bischöfliche Studienförderung Cusanuswerk to SM.

b) SM and AH: these authors have contributed equally to the studies presented in this manuscript.

c) Reprint requests:

Matthias U. Kassack, Institute of Pharmaceutical and Medicinal Chemistry, Pharmaceutical Biochemistry, Heinrich-Heine-University of Duesseldorf, Universitaetsstr. 1, Building 26.23.01, D-40225 Duesseldorf, Germany, Phone: +49-211-81 14587, Fax: +49-211-81 10801, e-mail: matthias.kassack@uni-duesseldorf.de

JPET Fast Forward. Published on October 8, 2009 as DOI: 10.1124/jpet.109.157750
This article has not been copyedited and formatted. The final version may differ from this version.

Legends for Figures

Fig. 1: Structural formulas of the $P2Y_{11}$ antagonist NF340 and the $P2Y_{11}$ agonist NF546.

Fig. 2. Functional characterisation of NF340.

Concentration-dependent inhibition by NF157 and NF340 of a response induced by injection of 1 µM ATPγS at $P2Y_{11}$ receptors in the calcium (**A**) and cAMP assay (**B**). Data shown are mean ± SEM of the pooled data of n > 3 experiments each with three replicates. Hill slopes were not significantly different from unity. pIC_{50} [NF157- Ca^{2+}] = 5.82 ± 0.05, pIC_{50} [NF340- Ca^{2+}] = 6.43 ± 0.04. pIC_{50} [NF157-cAMP] = 6.12 ± 0.04, pIC_{50} [NF340-cAMP] = 7.14 ± 0.06. **C** shows ATPγS concentration-response curves (calcium assay) at $P2Y_{11}$ receptors in the absence and presence of increasing concentrations of NF340. Data are mean ± SEM, n ≥ 5. **D** analyses the functional antagonist effect of NF340 (Schild plot). Dashed line shows 95% confidence interval. The highest single fluorescence (A, C) or luminescence (B) data point obtained in any of the n experiments by injection of 1 µM ATPγS (A, B) or 316 µM ATPγS (C) is set as 100% control.

Fig. 3. NF546 is a novel $P2Y_{11}$ agonist.

Concentration-response curves of ATPγS and NF546 at P2Y receptors using calcium (**A**) and cAMP assays (**B**). Hill coefficients were not significantly different from unity. **C** shows the inhibitory effect of 10 µM NF157 on the response of 1 µM ATPγS and 10 µM NF546 (calcium assay). Data shown are mean ± SEM of the pooled data of n > 3 experiments each with three replicates. The highest single fluorescence (A) or luminescence (B) data point of standard agonist controls obtained in any of the n experiments was set as 100% control. This was 100 µM ATPγS

for $P2Y_{11}$, 31.6 nM 2-MeSADP for $P2Y_1$, 1 μM UTP for $P2Y_2$ and $P2Y_4$, 1 μM UDP for $P2Y_6$, and 100 nM 2-MeSADP for $P2Y_{12}$, respectively.

Fig. 4. Functional characterisation of NF546.

A and **C** show concentration-response curves of NF546 at $P2Y_{11}$ receptors in the calcium (**A**) and cAMP assay (**C**) in the absence and presence of increasing concentrations of NF340. Data shown are representative for typical experiments out of three each with 3 replicates. **B** and **D** analyse the functional antagonist effect of NF340 shown in A or C, respectively (Schild plots). Dashed lines show 95% confidence intervals. The highest single fluorescence (A) or luminescence (C) data point obtained by injection of 316 μM ATPγS (A) or 100 μM ATPγS (C) is set as 100% control.

Fig. 5. Effect of P2 ligands on calcium signalling (A) and thrombospondin-1 secretion (B) in monocyte-derived dendritic cells. ATP, ATPγS, UTP, and NF546 were used in a concentration of 100 μM. Data are mean ± SD of three independent experiments. ATPγS-induced TSP-1 secretion was 1977 ng/ml.

Fig. 6. Effect of $P2Y_{11}$ ligands on cytokine release in human monocyte-derived dendritic cells. A shows a detail of a human proteome profiler cytokine array. Human monocyte-derived dendritic cells (DCs) were incubated with medium alone or medium containing 100 μM ATPγS or 100 μM NF546, respectively, for 24 h. **B** shows the inhibitory effect of 100 μM ATPγS and 100 μM NF546, respectively, on the LPS-induced release of IL-12p70 (ELISA) from DCs and the reversal of the ATPγS and NF546 effect by 10 μM NF340. Control is IL-12p70 concentration in medium supernatant from untreated cells. Data are mean ± SD of three independent experiments. **C** confirms the secretion of IL-8 (ELISA) induced by 10 μM ATPγS or 100 μM

NF546 respectively which was prevented by addition of 10 μM NF340. Basal control is IL-8 concentration in medium supernatant from untreated cells. Data are mean ± SD of three independent experiments.

Fig. 7. Putative binding site of the $P2Y_{11}$ receptor. A shows NF340, **B** shows NF546 docked into the ligand binding site. Ionic interactions and hydrogen bonds are shown as thin orange lines.

JPET Fast Forward. Published on October 8, 2009 as DOI: 10.1124/jpet.109.157750
This article has not been copyedited and formatted. The final version may differ from this version.

Tables

Table 1: Inhibition by 10 μM NF340 of standard agonist responses at P2Y receptors. Data shown are mean ± SD, n ≥ 3 independent experiments. Concentrations of agonists and pEC_{50} values are given in the Methods section.

Receptor	**% Inhibition**
$P2Y_1$	7.6 ± 12.9
$P2Y_2$	3.2 ± 4.1
$P2Y_4$	0.0 ± 6.9
$P2Y_6$	7.9 ± 17.6
$P2Y_{11}$	**93.1 ± 3.3**
$P2Y_{12}$	0.0 ± 7.0

Table 2: Potency (pEC_{50}) of NF546 at P2Y receptors (calcium assay). Data shown are mean ± SEM, n ≥ 3.

Receptor	**pEC_{50}**
$P2Y_1$	< 4
$P2Y_2$	4.82 ± 0.03
$P2Y_4$	< 4
$P2Y_6$	4.26 0.05
$P2Y_{11}$	**6.27 ± 0.07**
$P2Y_{12}$	3.49 ± 0.14

JPET Fast Forward. Published on October 8, 2009 as DOI: 10.1124/jpet.109.157750
This article has not been copyedited and formatted. The final version may differ from this version.

Table 3: Amino acid residues in the putative $P2Y_{11}$ receptor binding pocket contributing to the binding of NF340 and NF546.

Amino acid	Putative NF340 binding part	Putative NF546 binding part
Lys22	Sulfonic acid (ring1, pos.2)	-
Trp32	Sulfonic acid (ring1, pos.6)	-
Arg103	Sulfonic acid (ring2, pos.2)	Amide carbonyl
Arg106	Sulfonic acid (ring1, pos.6)	-
Thr110	Sulfonic acid (ring2, pos.2)	-
Thr164	Sulfonic acid (ring2, pos.2)	Phosphonate group (pos.1)
Arg184	Urea carbonyl	Amide carbonyl
Glu186	-	Urea NH
His265	Sulfonic acid (ring2, pos.6)	-
Arg268	Sulfonic acid (ring2, pos.6)	Phosphonate group (pos.3)
Arg307	Amide carbonyl; Sulfonic acid (ring1, pos.6)	-

JPET Fast Forward. Published on October 8, 2009 as DOI: 10.1124/jpet.109.157750
This article has not been copyedited and formatted. The final version may differ from this version.

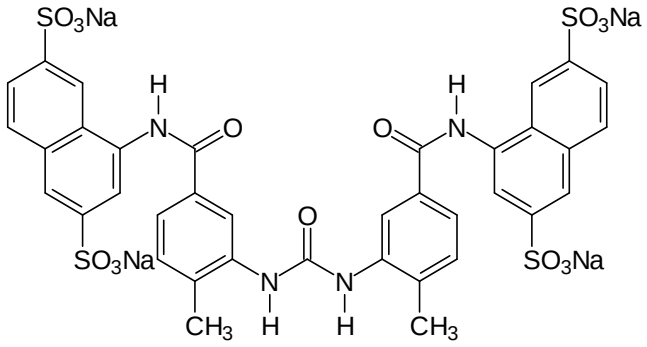

NF340

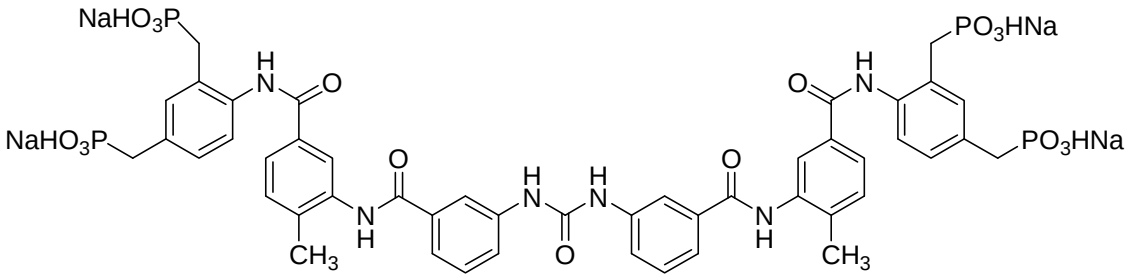

NF546

Fig.1

JPET Fast Forward. Published on October 8, 2009 as DOI: 10.1124/jpet.109.157750
This article has not been copyedited and formatted. The final version may differ from this version.

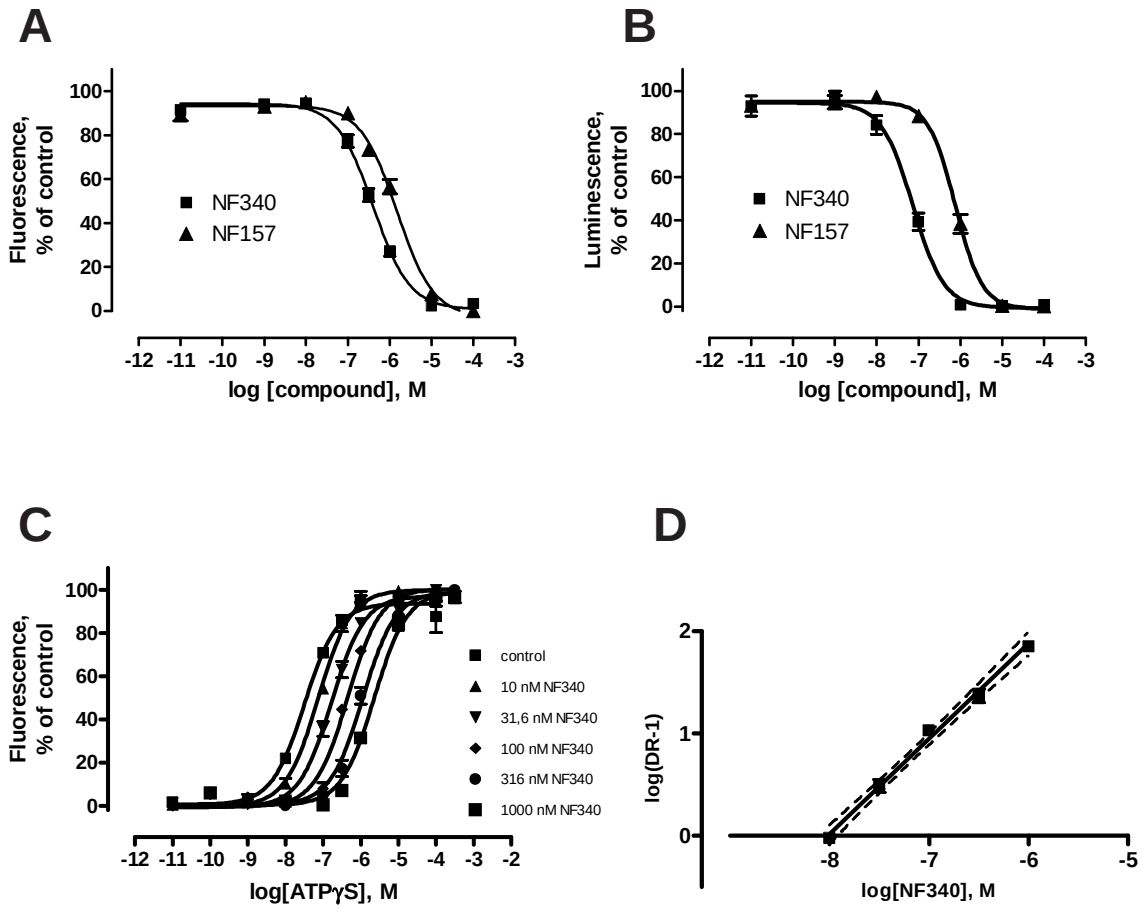

Fig. 2

JPET Fast Forward. Published on October 8, 2009 as DOI: 10.1124/jpet.109.157750
This article has not been copyedited and formatted. The final version may differ from this version.

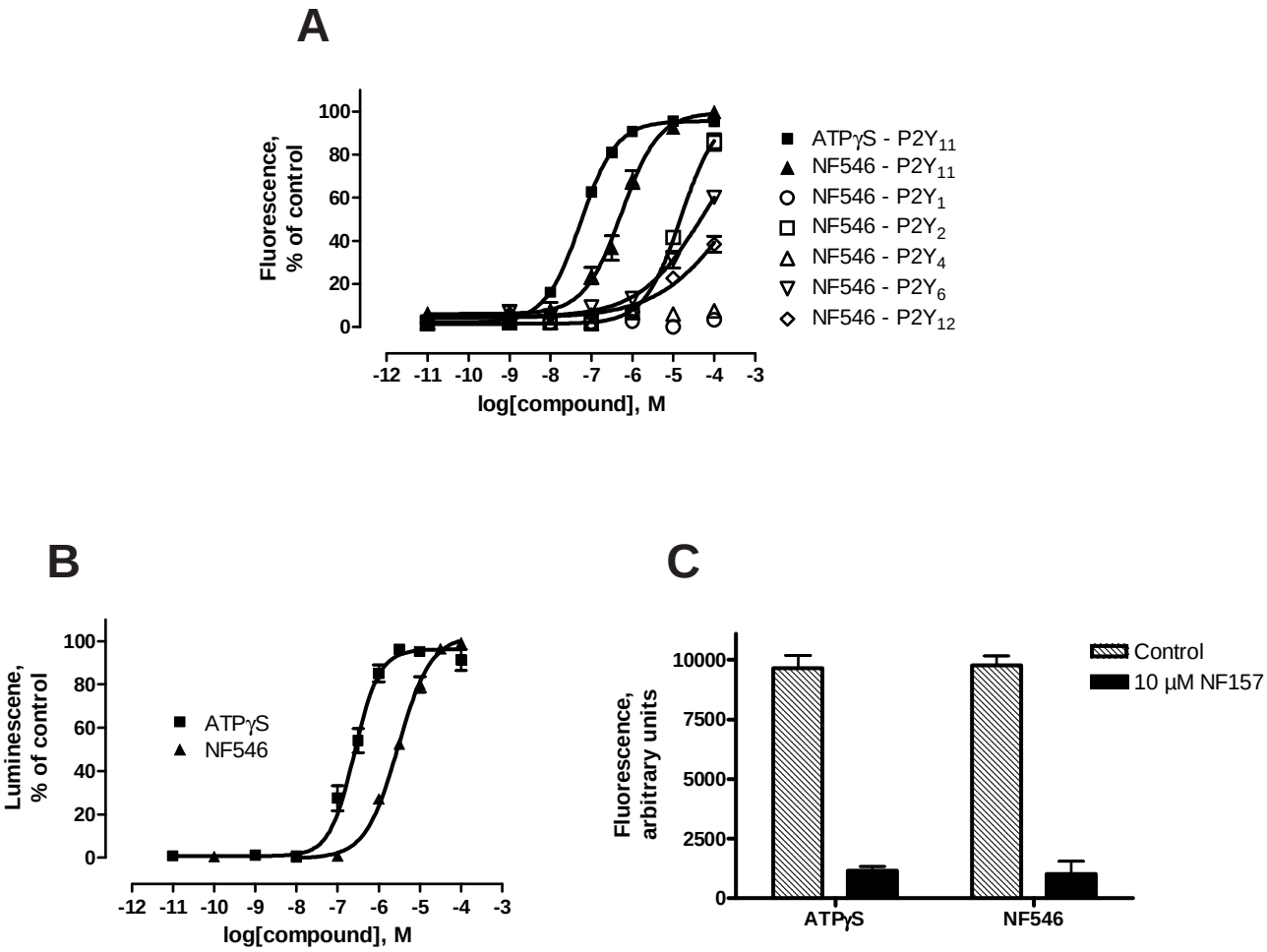

Fig. 3

JPET Fast Forward. Published on October 8, 2009 as DOI: 10.1124/jpet.109.157750
This article has not been copyedited and formatted. The final version may differ from this version.

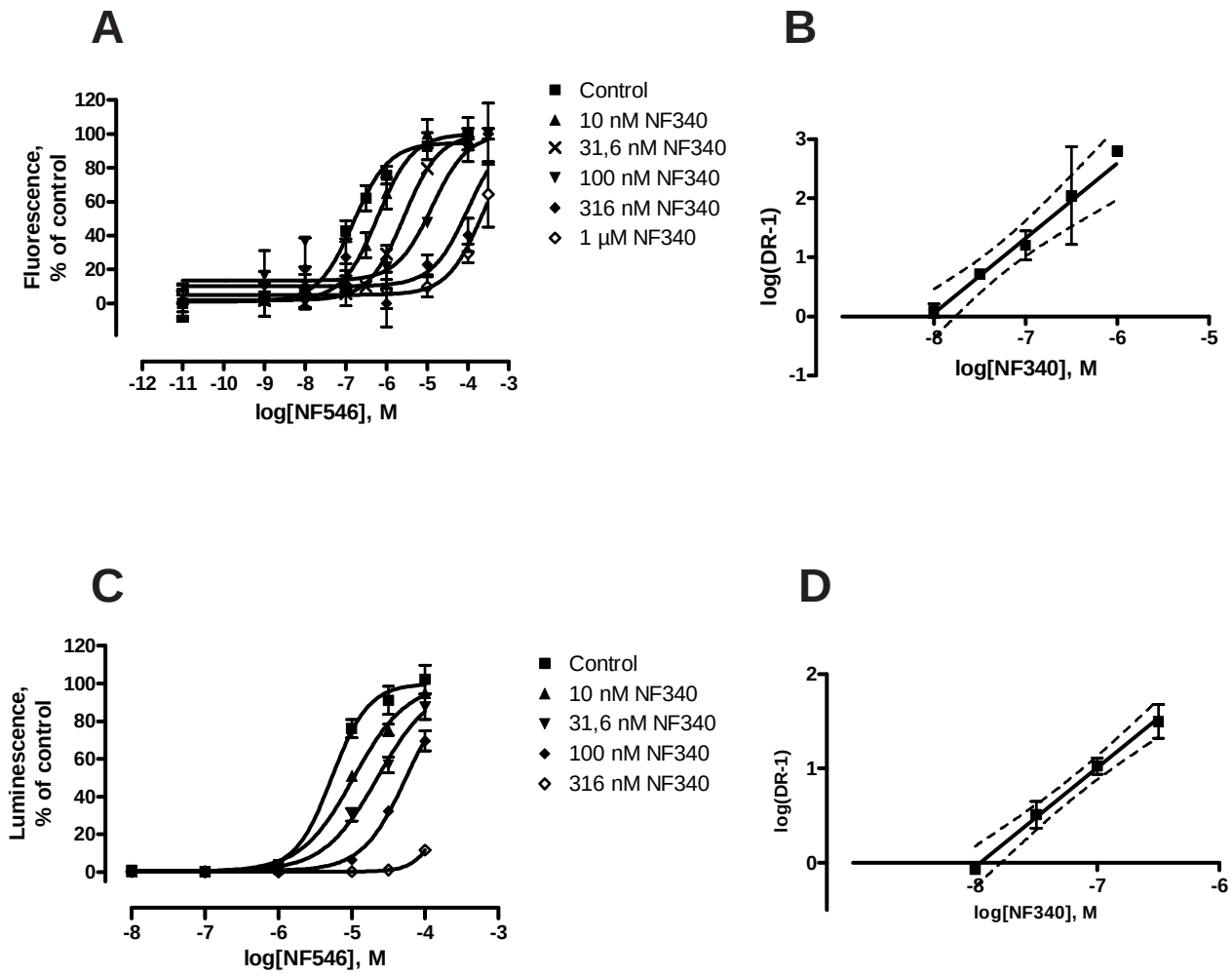

Fig. 4

JPET Fast Forward. Published on October 8, 2009 as DOI: 10.1124/jpet.109.157750
This article has not been copyedited and formatted. The final version may differ from this version.

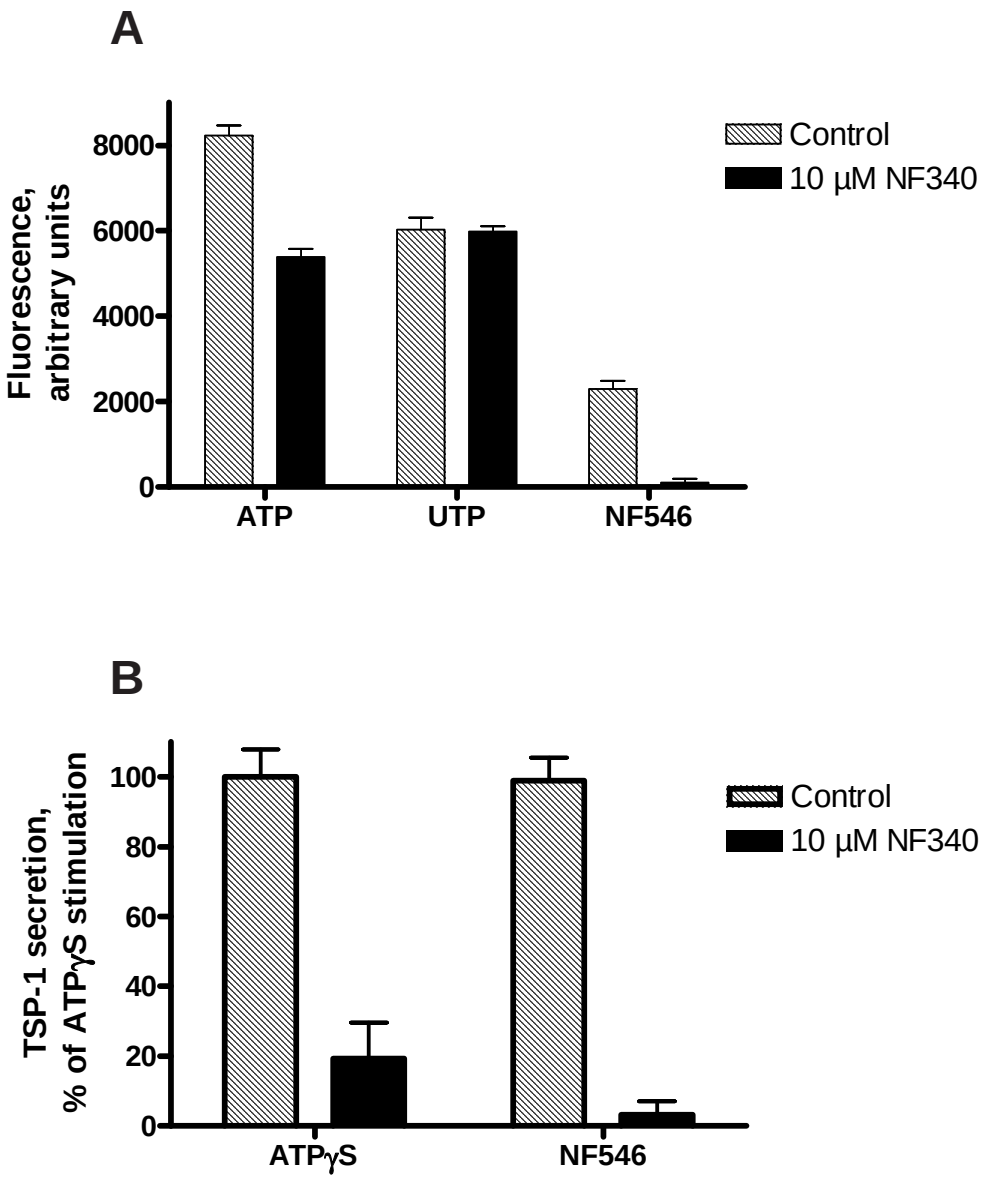

Fig. 5

JPET Fast Forward. Published on October 8, 2009 as DOI: 10.1124/jpet.109.157750
This article has not been copyedited and formatted. The final version may differ from this version.

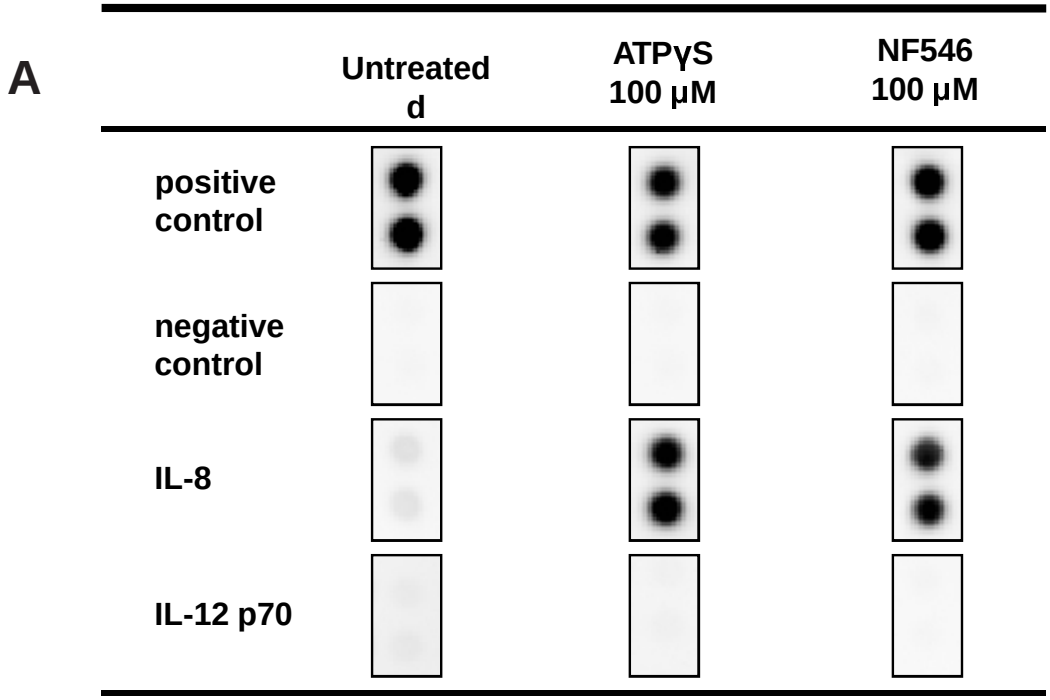

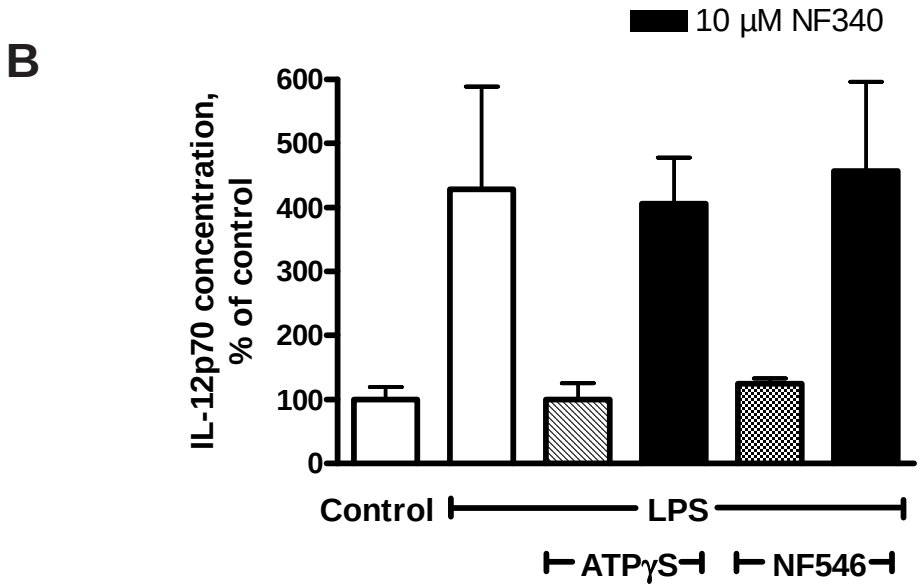

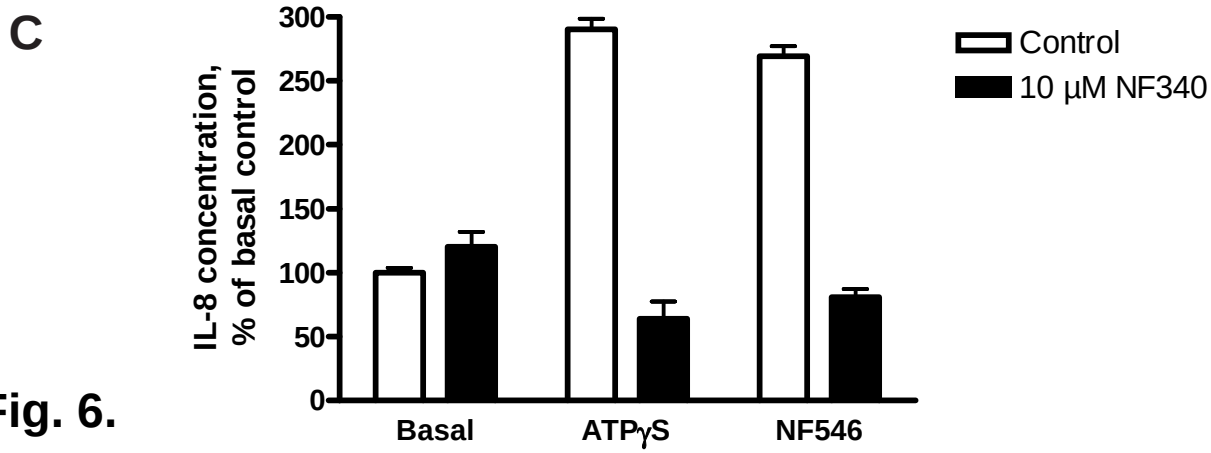

Fig. 6.

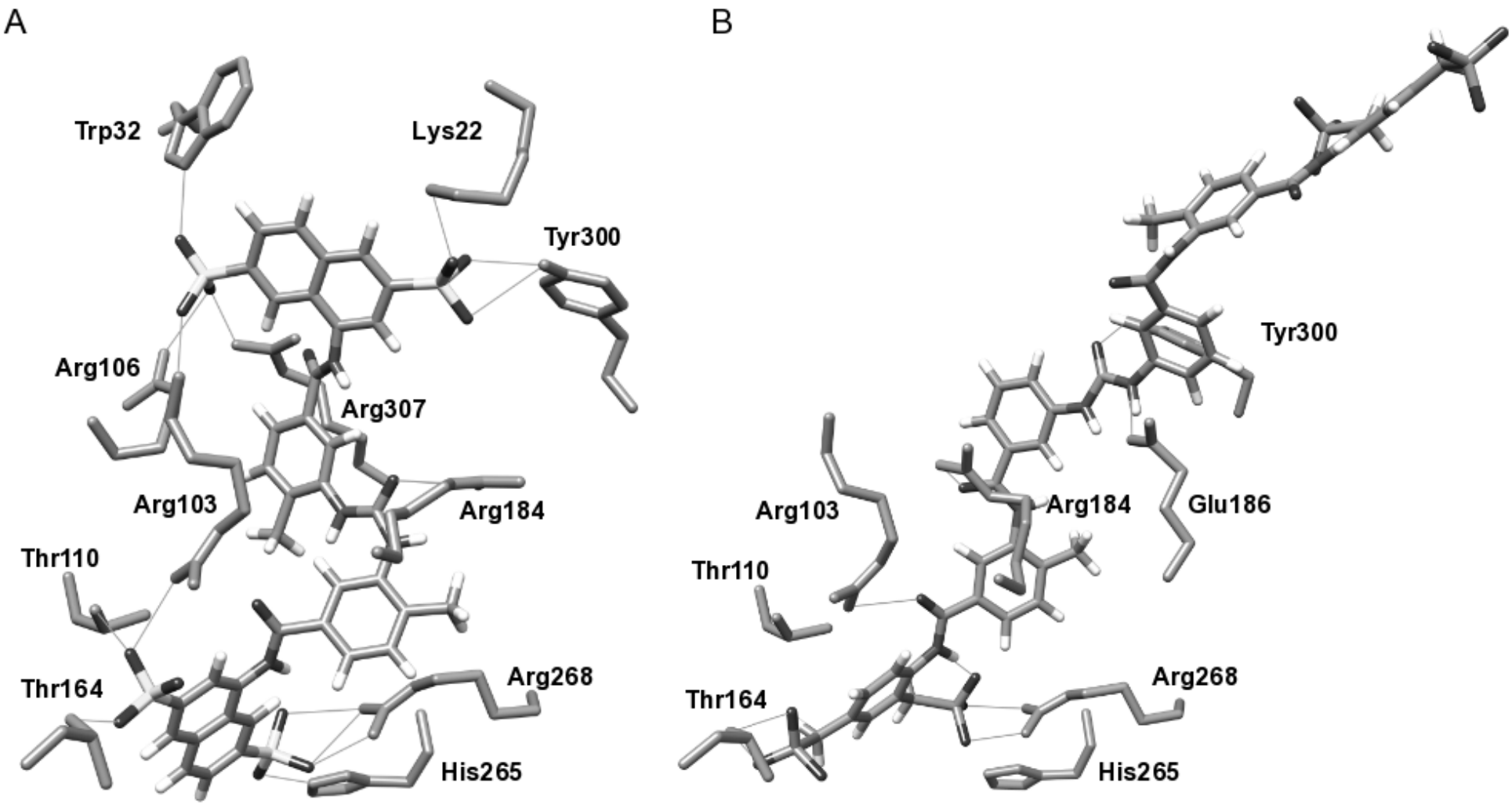

Fig. 7.